



HHS Public Access

Author manuscript

Bioconjug Chem. Author manuscript; available in PMC 2021 July 30.

Published in final edited form as:

Bioconjug Chem. 2020 October 21; 31(10): 2288–2292. doi:10.1021/acs.bioconjchem.0c00453.

***In Vivo* Targeting Using Arylboronate/Nopoldiol Click Conjugation**

Sandeep Palvai,

Joint Department of Biomedical Engineering, University of North Carolina - Chapel Hill and North Carolina State University Raleigh, Raleigh, North Carolina 27695, United States

Jasmine Bhangu,

Department of Chemistry, University of Alberta, Edmonton, Alberta T6G 2G2, Canada

Burcin Akgun,

Department of Chemistry, University of Alberta, Edmonton, Alberta T6G 2G2, Canada

Christopher T Moody,

Joint Department of Biomedical Engineering, University of North Carolina - Chapel Hill and North Carolina State University Raleigh, Raleigh, North Carolina 27695, United States

Dennis G Hall,

Department of Chemistry, University of Alberta, Edmonton, Alberta T6G 2G2, Canada

Yevgeny Brudno

Joint Department of Biomedical Engineering, University of North Carolina - Chapel Hill and North Carolina State University Raleigh, Raleigh, North Carolina 27695, United States

Abstract

Bioorthogonal click reactions yielding stable and irreversible adducts are in high demand for *in vivo* applications, including in biomolecular labeling, diagnostic imaging, and drug delivery. Previously, we reported a novel bioorthogonal “click” reaction based on the coupling of ortho-acetyl arylboronates and thiosemicarbazide-functionalized nopoldiol. We now report that a detailed structural analysis of the arylboronate/nopoldiol adduct by X-ray crystallography and ¹¹B NMR reveals that the bioorthogonal reactants form, unexpectedly, a tetracyclic adduct through the cyclization of the distal nitrogen into the semithiocarbazone leading to a strong B—N dative bond and two new 5-membered rings. The cyclization adduct, which protects the boronate unit against hydrolytic breakdown, sheds light on the irreversible nature of this polycondensation. The potential of this reaction to work in a live animal setting was studied through *in vivo* capture of

Corresponding Author: Yevgeny Brudno – ybrudno@ncsu.edu.

The authors declare no competing financial interest.

ASSOCIATED CONTENT

Supporting Information

The Supporting Information is available free of charge at <https://pubs.acs.org/doi/10.1021/acs.bioconjchem.0c00453>.

Experimental procedures and analysis (PDF)

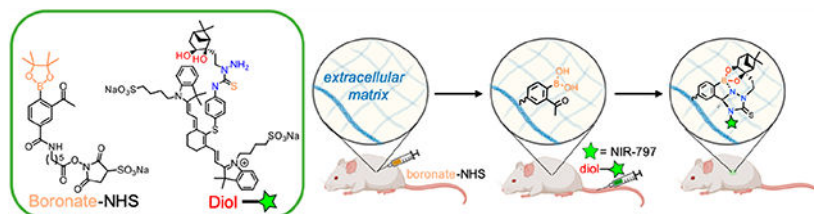
Crystallography report (CIF)

Structure report (PDF)

Complete contact information is available at: <https://pubs.acs.org/10.1021/acs.bioconjchem.0c00453>

fluorescently labeled molecules *in vivo*. Arylboronates were introduced into tissues through intradermal injection of their activated NHS esters, which react with amines in the extracellular matrix. Fluorescently labeled nopoldiol molecules were administered systemically and were efficiently captured by the arylboronic acids in a location-specific manner. Taken together, these *in vivo* proof-of-concept studies establish arylboronate/nopoldiol bioorthogonal chemistry as a candidate for wide array of applications in chemical biology and drug delivery.

Graphical Abstract



Chemistries capable of functioning inside live animals or humans are increasingly attracting attention for potential roles in basic science, diagnostics, and therapeutic application.^{1–9} In particular, bioorthogonal “click” reactions based on strain-promoted azide—alkyne chemistry (SPAAC) and inverse electron-demand Diels—Alder (iEDDA) have gained prominence due to the exquisite specificity between the reactive partners, fast reaction kinetics, high yields, and compatibility with physiological conditions.^{10–15}

Despite the significant success of SPAAC and iEDDA, new chemical strategies to physiological couplings are needed. Recently, we introduced a novel bioorthogonal click reaction between nopoldiol and ortho-substituted arylboronic acids.¹⁶ The reaction provides ligation kinetics ($\sim 9 \text{ M}^{-1} \text{ s}^{-1}$)¹⁶ that are an order of magnitude better than most SPAAC chemistries and similar to norbornene-based iEDDA chemistries, though far slower than TCO-based iEDDA.¹⁷ In this reaction, the product was stabilized through the introduction of a thiosemicarbazide to the nopoldiol, which forms a synergetic hydrazone linkage with an ortho-acetyl group designed strategically onto the arylboronic acid.^{16,18–20} Our initially proposed mechanism for this novel nopoldiol/arylboronate thiosemicarbazide/acetyl synergic (NAB—TAS) system leaves a trivalent boronic ester susceptible to hydrolysis, possibly leading to reversibility of the reaction, which was a potential limitation for widespread use of this click chemistry in complex, aqueous conditions, including in live animals.

RESULTS AND DISCUSSION

A deeper understanding of the mechanisms of product formation would provide insight for the future design of next-generation bioorthogonal reactions. With a view to pursue applications in cell-based and live bioconjugation, we sought to better understand the structure and properties of the NAB-TAS coupling. In previous studies, we proposed that ortho-acetyl phenylboronic acid and nopoldiol form a stable medium-sized ring product as a result of a triple condensation, affording two new rings with both a boronic ester and a thiosemicarbazone (Figure 1A).

To better understand the reaction mechanism, we characterized the adduct formed from model reagents **1** and **2** by X-ray crystallography and ^{11}B NMR spectroscopy. The planar trigonal boronic ester of putative adduct **3** was not observed. Instead, the resulting structure pointed to a tetrahedral boron species featuring an additional bond (d 1.76 Å) between the boron atom and one of the hydrazone nitrogens (Figure 1B). Presumably, due to its proximity to the C=N bond, the distal semithiocarbazone nitrogen atom in intermediate **3** cyclizes into the C=N carbon, which in turn leads to a strong B=N dative bond and two new 5-membered rings (Figure 1C). The formation of tetracyclic polycondensation adduct **4**, an isomer of **3**, is not merely a solid-state phenomenon; adduct **4** was analyzed by ^{11}B NMR spectroscopy in methanol (CD_3OD), which revealed a sharp singlet with a chemical shift of 13.8 ppm (Figure S1) consistent with a neutral tetrahedral boronate adduct. This new structural information, which concurs with the current understanding of B—N interactions,^{21,22} further explains the lack of reversibility observed in our initial studies.¹⁶ Although future efforts will be necessary to assess product stability in physiological environments such as in serum and tissues, we believe that the formation of a tetracyclic adduct with an internal tetrahedral B—N complex results in a boronate that is protected against hydrolysis,²³ making this click chemistry practically irreversible.

Inspired both by the stability of the reaction products and by the lack of toxicity of this compound in cells,¹⁶ we studied the *in vivo* feasibility of NAB—TAS coupling in live mice. We recently reported a fast and efficient method to interrogate click chemistry reactions *in vivo* without relying on complex biochemical integration. The method anchors click chemistry motifs directly at tissue sites by injecting water-soluble sulfo NHS-activated acyl groups at intradermal, intratumoral, and intracranial sites.²⁴ The activated esters react with amines on tissue extracellular matrix (ECM) and anchor the chemistry motifs locally at tissue sites. The click partner to be assessed is fluorescently labeled and administered systemically (i.e., intravascular) and fluorescence at the locally injected site assessed for evidence of *in vivo* click conjugation.²⁴

Testing the click chemistry *in vivo* necessitates the ECM-anchoring NHS ester and also a fluorescently labeled circulating partner. Due to synthetic accessibility, we chose to form the NHS ester of the boronate (**7**) and a fluorescent conjugate of the nopoldiol (**10**). The boronate was formulated as the pinacol boronic ester because it is easier to prepare and handle, is quickly hydrolyzed to the reactive boronic acid, and (as previously reported¹⁶) its presence does not impede the formation of biorthogonal adduct. The synthesis of arylboronate **6** from compound **5** proceeded as previously published except for the utilization the Fries rearrangement in place of Friedl—Crafts acylation, which provided a 33% increase in yield (see SI for compound **S4**). DCC coupling was used to provide boronate-sNHS **7** (Figure 2). The synthesis of fluorescently labeled nopoldiol (**10**) proceeded from previously published synthetic methods for nopoldiol. *cis*-Diol formation from the commercially available (–)-nopol (**8**) yielded compound **S1**, which was brominated to give bromide derivative **9**, as reported previously.¹⁶ Compound **9** was first functionalized with hydrazine, and then reacted with commercial fluorophore NIR-797 isothiocyanate to give compound **10** in 38% yield (Figure 2B).

In order to assess the NAB—TAS coupling in live animals, we studied whether intradermally injected arylboronates could capture systemically circulating nopoldiol—NIR (Figure 3A). boronate—NHS 7 was dissolved in phosphate—buffered saline (PBS) and injected intradermally on the flanks of outbred, CD1 mice. Intradermal PBS injections on a different location of the mouse flank served as a negative control. A small amount of ulceration was observed at the injection site 24 h after injection, but these lesions were not deemed burdensome by veterinary staff. We suspect that these lesions were caused by the injection of a partially precipitated solution of boronate—NHS, as previously observed for saturated solutions of azide— and tetrazine—NHS. Future studies will further study the *in vivo* biocompatibility of these “click” chemistry motifs. Twenty-four hours after intradermal injection, diol—NIR was retro-orbitally administered and *in vivo* fluorescence was monitored at both the boronate—NHS and PBS injection sites over 1 week. Both immediately and 3 h after i.v. administration, diol—NIR fluorescence was observed throughout the animal’s body (Figure S2). However, as the fluorescent molecule was cleared from the animal’s body, the fluorescence slowly localized to the boronate—NHS injection site, but not to the PBS control injection site (Figure 3B). After 24 h, ECM-anchored arylboronates captured significantly more fluorescent signal as compared to PBS (Figure 3C), suggesting that the circulating diol-NIR was being captured by boronate—NHS selectively via click chemistry. Since the ulceration may enhance signal from any remaining blood-circulating fluorophores, we repeated the imaging at 7 days, at which point fluorophores will be cleared from the circulation and the ulcerations have healed. The statistically significant difference between boronate—NHS and control PBS persisted over 1 week, further supporting the stability of adduct (Figure 3C) *in vivo*.

CONCLUSION

Taken together, this work reports new X-ray crystallographic, boron NMR, and *in vivo* capturing data demonstrating the promise of NAB—TAS coupling for a vast array of *in vivo* applications. Contrary to the initially hypothesized bicyclic adduct, the product of the click polycondensation chemistry reacts further to form an isomeric tetracyclic hydrazino—boronate adduct, which explains the stability and apparent irreversibility of this bioorthogonal reaction. Further, this click reaction adduct was amenable to *in vivo* application. In particular, anchored arylboronate motifs captured systemically circulating fluorescent nopoldiol reagents. We believe these findings will be broadly useful to the future development of next-generation boronate-based bioorthogonal click reactions in biomedical application. *In vivo* observations proved that this novel click chemistry has the potential to be applied in living systems and to serve as a valuable addition to the bioorthogonal chemistry toolkit for *in vivo* molecular labeling, imaging, and drug delivery.

Supplementary Material

Refer to Web version on PubMed Central for supplementary material.

ACKNOWLEDGMENTS

The authors are grateful to the NC State veterinary staff for proper care of animals used in experiments and valuable resources on training. We thank Dr. Michael Ferguson (X-ray Crystallography Laboratory, University of Alberta)

for the X-ray crystallographic analysis of compound **4**, and Mr. Ed Fu (University of Alberta) for support in the HPLC analysis and purification of conjugates. This work was supported by the National Center for Advancing Translational Sciences (NCATS), National Institutes of Health, through Grant Award Number UL1TR002489, by the UNC Lineberger Comprehensive Cancer Center's University Cancer Research Fund, by a Faculty Research and Professional Development Grant from North Carolina State University, by the Natural Sciences and Engineering Research Council (NSERC) of Canada (Discovery Grant to DGH), the University of Alberta, and by start-up funds from the University of North Carolina and North Carolina State University. B.A. thanks Alberta Innovates—Technology Futures for a Graduate Scholarship.

REFERENCES

- (1). Thirumurugan P, Matosiuk D, and Jozwiak K (2013) Click Chemistry for Drug Development and Diverse Chemical—Biology Applications. *Chem. Rev.* 113 (7), 4905–4979. [PubMed: 23531040]
- (2). Kenry, and Liu B. (2019) Bio-Orthogonal Click Chemistry for In Vivo Bioimaging. *Trends in Chemistry* 1 (8), 763–778.
- (3). Mushtaq S, Yun S-J, and Jeon J (2019) Recent Advances in Bioorthogonal Click Chemistry for Efficient Synthesis of Radiotracers and Radiopharmaceuticals. *Molecules* 24 (19), 3567.
- (4). Liang D, Wu K, Tei R, Bumpus TW, Ye J, and Baskin JM (2019) A Real-Time, Click Chemistry Imaging Approach Reveals Stimulus-Specific Subcellular Locations of Phospholipase D Activity. *Proc. Natl. Acad. Sci. U. S. A.* 116 (31), 15453–15462. [PubMed: 31311871]
- (5). Yoon HY, Koo H, Kim K, and Kwon IC (2017) Molecular Imaging Based on Metabolic Glycoengineering and Bioorthogonal Click Chemistry. *Biomaterials* 132, 28–36. [PubMed: 28399460]
- (6). Baskin JM, Prescher JA, Laughlin ST, Agard NJ, Chang PV, Miller IA, Lo A, Codelli JA, and Bertozzi CR (2007) Copper-Free Click Chemistry for Dynamic in Vivo Imaging. *Proc. Natl. Acad. Sci. U. S. A.* 104 (43), 16793–16797. [PubMed: 17942682]
- (7). Brudno Y, Ennett-Shepard AB, Chen RR, Aizenberg M, and Mooney DJ (2013) Enhancing Microvascular Formation and Vessel Maturation through Temporal Control over Multiple Pro-Angiogenic and pro-Maturation Factors. *Biomaterials* 34 (36), 9201–9209. [PubMed: 23972477]
- (8). Brudno Y, Desai RM, Kwee BJ, Joshi NS, Aizenberg M, and Mooney DJ (2015) In Vivo Targeting through Click Chemistry. *ChemMedChem* 10 (4), 617–620. [PubMed: 25704998]
- (9). Zou L, Braegelman AS, and Webber MJ (2019) Spatially Defined Drug Targeting by in Situ Host-Guest Chemistry in a Living Animal. *ACS Cent. Sci.* 5 (6), 1035–1043. [PubMed: 31263763]
- (10). Takayama Y, Kusamori K, and Nishikawa M (2019) Click Chemistry as a Tool for Cell Engineering and Drug Delivery. *Molecules* 24 (1), 172.
- (11). McKay CS, and Finn MG (2014) Click Chemistry in Complex Mixtures: Bioorthogonal Bioconjugation. *Chem. Biol.* 21 (9), 1075–1101. [PubMed: 25237856]
- (12). Lim RKV, and Lin Q (2010) Bioorthogonal Chemistry—A Covalent Strategy for the Study of Biological Systems. *Sci. China: Chem.* 53 (1), 61–70. [PubMed: 20694042]
- (13). Devaraj NK (2018) The Future of Bioorthogonal Chemistry. *ACS Cent. Sci.* 4 (8), 952–959. [PubMed: 30159392]
- (14). Oliveira BL, Guo Z, and Bernardes GJL (2017) Inverse Electron Demand Diels—Alder Reactions in Chemical Biology. *Chem. Soc. Rev.* 46 (16), 4895–4950. [PubMed: 28660957]
- (15). Debets MF, van der Doelen CWJ, Rutjes FPJT, and van Delft FL (2010) Azide: A Unique Dipole for Metal-Free Bioorthogonal Ligations. *ChemBioChem* 11 (9), 1168–1184. [PubMed: 20455238]
- (16). Akgun B, Li C, Hao Y, Lambkin G, Derda R, and Hall DG (2017) Synergic “Click” Boronate/Thiosemicarbazone System for Fast and Irreversible Bioorthogonal Conjugation in Live Cells. *J. Am. Chem. Soc.* 139 (40), 14285–14291. [PubMed: 28891646]
- (17). Patterson DM, Nazarova LA, and Prescher JA (2014) Finding the Right (Bioorthogonal) Chemistry. *ACS Chem. Biol.* 9 (3), 592–605. [PubMed: 24437719]
- (18). Akgun B, and Hall DG (2018) Boronic Acids as Bioorthogonal Probes for Site-Selective Labeling of Proteins. *Angew. Chem., Int. Ed.* 57 (40), 13028–13044.

- (19). Cambray S, and Gao J (2018) Versatile Bioconjugation Chemistries of Ortho-Boronyl Aryl Ketones and Aldehydes. *Acc. Chem. Res.* 51 (9), 2198–2206. [PubMed: 30110146]
- (20). António JPM, Russo R, Carvalho CP, Cal PMSD, and Gois PMP (2019) Boronic Acids as Building Blocks for the Construction of Therapeutically Useful Bioconjugates. *Chem. Soc. Rev.* 48 (13), 3513–3536. [PubMed: 31157810]
- (21). Antonio JPM, Farias GDV, Santos FMF, Oliveira R, Pedro MS, and Gois PMP. Boron-Nitrogen Bond. In *Non-covalent Interactions in the Synthesis and Design of New Compounds*, 2016; pp 23–48. DOI: 10.1002/9781119113874.ch2.
- (22). Dong H, Li W, Sun J, Li S, and Klein ML (2015) Understanding the Boron-Nitrogen Interaction and Its Possible Implications in Drug Design. *J. Phys. Chem. B* 119 (45), 14393–14401. [PubMed: 26473577]
- (23). Hall DG Introduction: Properties, Preparation, Overview of Application. In *Boronic Acids, Preparation and Applications in Organic Synthesis, Medicine and Materials*; John Wiley & Sons, 2011. DOI: 10.1002/9783527639328.ch1.
- (24). Adams MR, Moody CT, Sollinger JL, and Brudno Y (2019) Extracellular-Matrix-Anchored Click Motifs for Specific Tissue Targeting. *Mol. Pharmaceutics* 17 (2), 392–403.

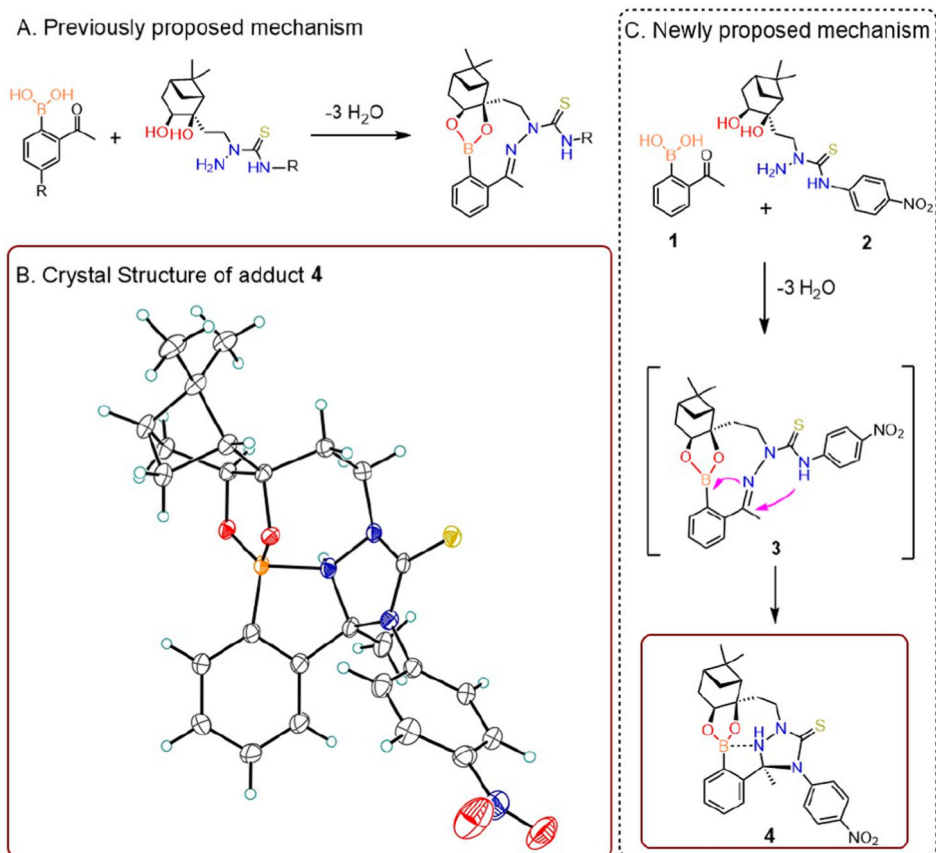
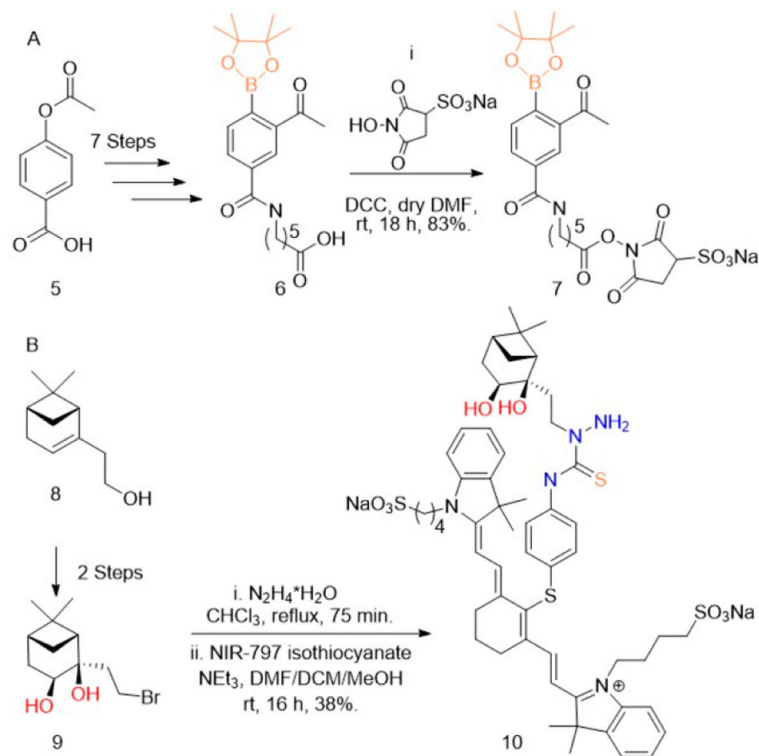


Figure 1. Formation and characterization of crystal structure of the bioorthogonal adduct in NAB—TAS coupling. (A) Previously proposed reaction mechanism with a planar trigonal boronic ester adduct. (B) ORTEP representation of crystallographic analysis of the reaction adduct (4). (C) Newly proposed mechanism incorporating double condensation reaction.

**Figure 2.**

Synthesis of boronate—sNHS and nopolydiol—NIR. Reagents and conditions: (A) **6** was synthesized over seven steps from **5** (see Supporting Information (SI)). (i) sulfoNHS (0.9 equiv), DCC (1 equiv) dry DMF (1 mL), rt, 18 h, 83%. (B) **9** was synthesized over two steps from **8** (see SI). (i) N₂H₄·H₂O (20 equiv) CHCl₃ (1.0 mL) reflux, 75 min. (ii) NIR-797 isothiocyanate (1 equiv), NEt₃ (1.2 equiv), DMF/DCM/MeOH (5:5:1), rt, 16 h, 38%.

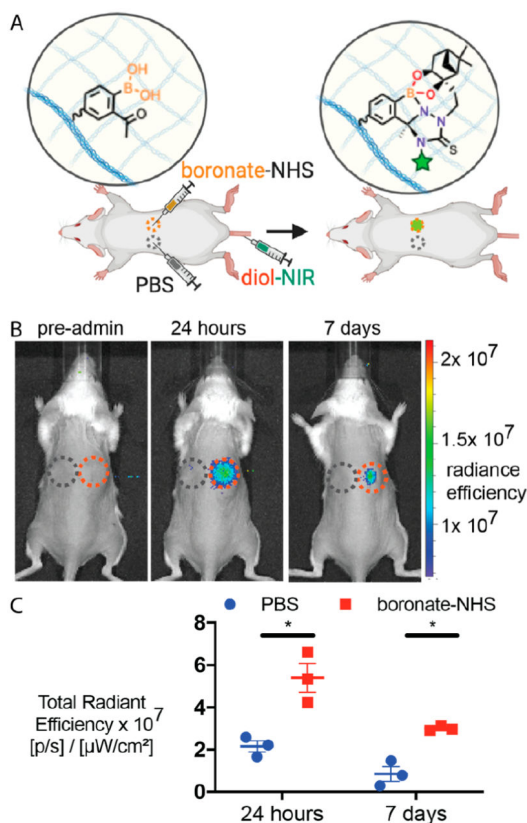


Figure 3.

In vivo validation of NAB—TAS coupling. (A) Schematic image of experiment. Boronic acids are anchored to tissue ECM and fluorescent diol is administered i.v. for click capture. (B) Representative IVIS images of mice before and 1 week after systemic administration of diol—NIR. Blue and red dashed circles indicate PBS and boronate—NHS injection sites, respectively. (C) Quantitation of fluorescence signal at injection site 24 h and 1 week after systemic administration of diol—NIR. Mean \pm SEM ($N=3$). Statistical significance was measured using a paired, one-tailed Student's *t* test and represented as $*p < 0.05$. For full IVIS images of all mice at 0, 3, and 24 h and 7 days, see Figure S2.